

UCAD: UNCERTAINTY-GUIDED CONTOUR-AWARE DISPLACEMENT FOR SEMI-SUPERVISED MEDICAL IMAGE SEGMENTATION

Chengbo Ding^{1,2}, Fenghe Tang^{1,2}, and Shaohua Kevin Zhou^{1,2,3,4*}

¹ School of Biomedical Engineering, Division of Life Sciences and Medicine,

University of Science and Technology of China (USTC), Hefei, Anhui 230026, China

² Center for Medical Imaging, Robotics, Analytic Computing & Learning (MIRACLE), Suzhou Institute for Advanced Research, USTC, Suzhou, Jiangsu 215123, China

³ Jiangsu Provincial Key Laboratory of Multimodal Digital Twin Technology, Suzhou Jiangsu, 215123, China

⁴ State Key Laboratory of Precision and Intelligent Chemistry, USTC, Hefei Anhui 230026, China

ABSTRACT

Existing displacement strategies in semi-supervised segmentation only operate on rectangular regions, ignoring anatomical structures and resulting in boundary distortions and semantic inconsistency. To address these issues, we propose **UCAD**, an *Uncertainty-Guided Contour-Aware Displacement* framework for semi-supervised medical image segmentation that preserves contour-aware semantics while enhancing consistency learning. Our UCAD leverages superpixels to generate anatomically coherent regions aligned with anatomy boundaries, and an uncertainty-guided selection mechanism to selectively displace challenging regions for better consistency learning. We further propose a dynamic uncertainty-weighted consistency loss, which adaptively stabilizes training and effectively regularizes the model on unlabeled regions. Extensive experiments demonstrate that UCAD consistently outperforms state-of-the-art semi-supervised segmentation methods, achieving superior segmentation accuracy under limited annotation. The code is available at: <https://github.com/dcb937/UCAD>.

Index Terms— Semi-supervised learning, Medical image segmentation, Uncertainty estimation, Contour-aware displacement

1. INTRODUCTION

Medical image segmentation is crucial yet heavily constrained by limited annotations [1, 2, 3, 4, 5, 6]. Semi-supervised learning (SSL) has thus become a key approach to reduce labeling costs and enhance generalization [7]. Most existing SSL methods can be categorized into three types: Input perturbations [8, 9, 10, 11, 12], model perturbations [13, 1, 14], and feature perturbations [15, 16]. Among them, input perturbations aim to enhance the model’s robustness by altering the input images while preserving their

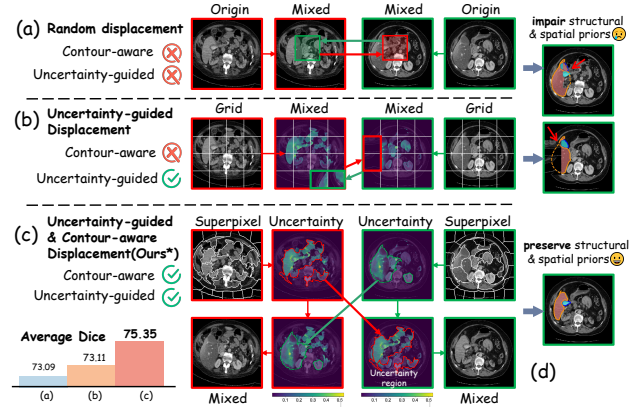


Fig. 1. Illustration of different displacement strategies: (a) **Random displacement**: randomly exchanges rectangular regions between labeled and unlabeled images, ignoring anatomical boundaries; (b) **Uncertainty-guided displacement**: divides images into grid patches and performs uncertainty-guided region exchange, but still lacks structural alignment; (c) **Uncertainty-guided contour-aware displacement (ours)**: generates superpixel-based, anatomically coherent regions and selectively displaces uncertain superpixel regions; (d) Comparing displacement results, we observe that conventional methods often impair structural and spatial priors, while our method maintains this information.

semantic content [8]. In recent years, region-level mixing methods [10, 14, 17] have become representative approaches within this category. Such strategies not only augment the data but also help alleviate the distribution mismatch between labeled and unlabeled samples [10]. From a broader view, these methods can be divided into (i) **Random displacement**, which performs random bidirectional copy–paste between labeled and unlabeled samples (e.g., BCP [10], in Fig. 1(a)) and (ii) **Uncertainty-guided displacement**, partitions images into non-overlapping grids and conducts uncertainty-guided

region exchange to encourage semantic complementarity (e.g., ABD [17], in Fig. 1(b)).

Despite their effectiveness, both random displacement and uncertainty-guided displacement share an inherent limitation: *they operate exclusively on rectangular regions and neglect the importance of preserving shape information essential for accurate anatomy understanding* [18] (Fig. 1(a, b, and d)). Anatomical structures in medical images typically exhibit irregular and curved boundaries. As shown in Fig. 1(d), when such rigid regions are copied or displaced, they may intersect anatomy contours unnaturally, leading to boundary distortions and semantic ambiguity. Moreover, uncertainty-guided rectangular regions displacement inadvertently relocates anatomically inconsistent regions, thereby disrupting semantic coherence and hindering the model’s ability to capture accurate structural and spatial representations. Such neglect restricts the model’s ability to capture shape-aware and semantically continuous representations, essential for accurate anatomical understanding. This motivates a key question: *Can we retain these shape-aware semantics while still benefiting from region displacement strategies?*

To address this challenge, we propose a novel **uncertainty-guided contour-aware displacement** strategy, as shown in Fig. 1(c). Aiming to enhance the model’s contour-aware perception of anatomical structures, our method utilizes unsupervised superpixels to form spatially coherent, boundary-preserving regions that align with anatomical boundaries. By displacing these semantically meaningful regions between images, our approach generates mixed samples that preserve both the anatomical shape and contextual information of anatomy, ensuring that structural cues are maintained while enhancing data diversity. In addition, to identify which regions require displacement, we incorporate uncertainty estimation to selectively perturb ambiguous or low-confidence areas, typically near anatomical boundaries. By focusing perturbations on these high-uncertainty regions, the model is encouraged to refine vague contours and learn sharper boundary representations, leading to improved structural and spatial robustness in consistency learning. Moreover, we design a dynamic uncertainty-weighted consistency loss which adaptively stabilizes training and enhances meaningful regularization specifically for unlabeled regions. Extensive experiments demonstrate that our approach achieves state-of-the-art performance compared with recent methods.

2. METHOD

The overall framework of our proposed method is illustrated in Fig. 2. Our approach is designed based on Mean Teacher [8]. We propose a contour-aware partition strategy for region-level mixing guided by superpixels, along with an uncertainty-driven displacement mechanism that prioritizes the replacement of difficult-to-learn regions to enhance supervision on challenging boundaries. Additionally, we employ

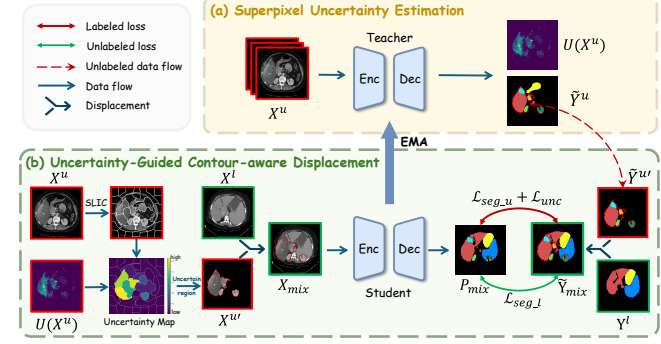


Fig. 2. Overview of our framework. (a) The teacher network takes the unlabeled image X^u as input to generate a pseudo label \tilde{Y}^u and a pixel-wise uncertainty score $U(X^u)$. (b) The unlabeled image X^u is partitioned into superpixel region using the SLIC [19] algorithm, and the uncertainty $U(X^u)$ guides the selection of N uncertain regions to form the mask \mathcal{M} . The masked regions are then displaced with the labeled image X^l , resulting in a mixed image X_{mix} and its corresponding mixed label \tilde{Y}_{mix} . The student network is trained on X_{mix} to predict P_{mix} , which is supervised by \tilde{Y}_{mix} and an uncertainty-weighted consistency loss \mathcal{L}_{unc} . For simplicity, the reverse displacement process is omitted.

a hybrid loss function that integrates supervised, consistency, and uncertainty-regularized terms.

2.1. Uncertainty-Guided Contour-Aware Displacement

Contour-Aware Partition. In order to improve the ability to capture anatomical contours under the semi-supervised setting, we introduce a contour-aware partition strategy guided by superpixels. The core idea is to replace selected superpixel regions from one image with the corresponding regions from another image, thereby generating mixed samples that preserve local structural consistency. Specifically, we adopt the Simple Linear Iterative Clustering (SLIC) [19] algorithm for creating superpixel regions: Let $\mathbf{X} \in \mathbb{R}^{H \times W}$ denote an input images with its corresponding labels $\mathbf{Y} \in \{0, 1, \dots, C-1\}^{H \times W}$, where C is the number of classes. Given a superpixel segmentation function $\mathcal{S}(\cdot)$, image \mathbf{X} can be decomposed into a set of K superpixel regions:

$$\mathcal{S}(\mathbf{X}) = \{s_1, s_2, \dots, s_K\}, \quad \bigcup_{k=1}^K s_k = \Omega, \quad s_i \cap s_j = \emptyset \quad (i \neq j), \quad (1)$$

where Ω denotes the entire image domain and s_k is a connected region of homogeneous appearance.

Uncertainty-Guided Displacement. Instead of sampling superpixel regions uniformly at random, we exploit the model’s predictive uncertainty to determine which regions should be replaced during mixing. Specifically, given the probability map produced by the teacher network, we compute the pixel-

wise Shannon entropy $H(\mathbf{X})$ [20]. For each superpixel s , the uncertainty score is obtained as the mean entropy within the region, and then transformed into a categorical distribution using a temperature-scaled softmax:

$$U(s) = \frac{1}{|s|} \sum_{x \in s} H(\mathbf{X}), \quad (2)$$

$$\mathcal{P}(s) = \frac{\exp(U(s)/T)}{\sum_{s'} \exp(U(s')/T)}, \quad (3)$$

where T is the temperature parameter controlling the sharpness of the distribution, and $s' \in \mathcal{S}$ denotes all superpixels in the current image.

Let $\mathcal{S}_N \sim \text{Categorical}(\mathcal{P}(s))$ denotes the set of the N uncertain superpixels regions which is sampled according to the probability distribution $\mathcal{P}(s)$. The corresponding mask is generated by setting the selected regions to one while leaving other regions as zero:

$$\mathbf{M}(\mathbf{X}) = \begin{cases} 1, & x \in \mathcal{S}_N, \\ 0, & \text{otherwise.} \end{cases} \quad (4)$$

Then we define two input images X_a and X_b sampled from the labeled and unlabeled sets (in either order). Let $\mathcal{M} = \mathbf{M}(\mathbf{X}_a)$ be the selected mask. The mixed image $\tilde{\mathbf{X}}$ and its label $\tilde{\mathbf{Y}}$ can be generated as follows:

$$\tilde{\mathbf{X}} = \mathcal{M} \odot \mathbf{X}_a + (1 - \mathcal{M}) \odot \mathbf{X}_b, \quad (5)$$

$$\tilde{\mathbf{Y}} = \mathcal{M} \odot \mathbf{Y}_a + (1 - \mathcal{M}) \odot \mathbf{Y}_b, \quad (6)$$

where \odot denotes the element-wise multiplication. Our method leverages the structural prior provided by superpixels, ensuring that the mixed regions better align with object boundaries. Building upon this, the uncertainty-guided selection mechanism ensures that highly uncertain regions, which are more difficult to learn, are preferentially replaced during displacement, thereby enhancing structural supervision and enabling more accurate contour representation.

2.2. The Overall Loss Function

Region-Level Hybrid Loss. To optimize the network, we adopt a hybrid loss function design that follows the design of BCP [10]. The overall objective integrates supervised loss on labeled regions, consistency loss on unlabeled regions, and an additional uncertainty-aware regularization. Given a segmentation prediction $\tilde{\mathbf{Y}}$ for the mixed image $\tilde{\mathbf{X}}$, a labeled target \mathbf{Y}_l , a pseudo label \mathbf{Y}_p for the unlabeled image, and a binary mask \mathcal{M} indicating whether the region comes from the labeled image, we define a combinational loss as follows:

$$\begin{aligned} \mathcal{L}_{seg} = & w_l \cdot \mathcal{L}_{DiceCE}(\tilde{\mathbf{Y}}, \mathbf{Y}_l; \mathcal{M}) \\ & + w_u \cdot \mathcal{L}_{DiceCE}(\tilde{\mathbf{Y}}, \mathbf{Y}_p; 1 - \mathcal{M}) \end{aligned} \quad (7)$$

where \mathcal{L}_{DiceCE} is the linear combination of Dice loss and Cross-entropy loss, and w_l, w_u are weights for labeled and unlabeled regions, respectively.

Dynamic Uncertainty-Weighted Loss. Inspired by the uncertainty-regularized consistency mechanism introduced in DyCON [21], we encourage the student prediction \mathbf{p}_s to be consistent with the teacher prediction \mathbf{p}_t to further regularize the model on unlabeled regions, while adaptively weighting the discrepancy according to predictive uncertainty. Specifically, the predictive entropy of both models, defined as the Shannon entropy over class probabilities, is used to adaptively weight the consistency discrepancy. The uncertainty-guided consistency loss is formulated as:

$$\begin{aligned} \mathcal{L}_{unc} = & \frac{1}{\mathcal{N}_u} \sum_{x \in \Omega_u} \frac{\|\mathbf{p}_s(x) - \mathbf{p}_t(x)\|^2}{\exp(\beta H_s(x)) + \exp(\beta H_t(x))} \\ & + \frac{\beta}{\mathcal{N}_u} \sum_{x \in \Omega_u} (H_s(x) + H_t(x)), \end{aligned} \quad (8)$$

where Ω_u denotes the unlabeled region, and $\mathcal{N}_u = |\Omega_u|$ is the number of voxels within it. $H_s(x)$ and $H_t(x)$ represent the predictive entropy of the student and teacher models. The coefficient β serves as an adaptive weighting factor that is gradually annealed during training. Finally, the total loss is defined as the weighted sum of all components:

$$\mathcal{L}_{total} = \mathcal{L}_{seg} + \lambda \cdot \mathcal{L}_{unc}, \quad (9)$$

where λ is a hyper-parameter balancing uncertainty regularization against supervised segmentation losses. This formulation ensures that the model benefits from both labeled supervision and unlabeled consistency.

3. EXPERIMENTS AND RESULTS

3.1. Experimental Setup

Dataset and Setting. We conduct experiments on two publicly datasets: ACDC [22] and Synapse [23]. **ACDC:** The Automated Cardiac Diagnosis Challenge (ACDC) dataset consists of cine-MRI scans acquired from 100 patients with different cardiac conditions. Following [10], we use the same dataset split with 70 training, 10 validation, and 20 testing samples. **Synapse:** The Synapse multi-organ CT dataset consists of 30 cases with 3,779 axial abdominal CT slices, each annotated for eight abdominal organs. We split 18, 6, and 6 cases for training, validation, and testing, respectively.

Implementation Details and Evaluation Metrics. Following previous works [10, 17], the input image size and patch size are set as 256×256 and the batch size is 24 during the training period. We use U-Net [24] as the backbone networks and the SGD optimizer with weight decay of 1e-4, momentum of 0.9, learning rate of 0.01, followed same setting as [10, 17]. We conduct all experiments on an NVIDIA GeForce 4090

Method	5% label		10% label	
	DSC(%) \uparrow	ASD \downarrow	DSC(%) \uparrow	ASD \downarrow
UA-MT [9]	46.04	7.75	81.65	2.12
SASSNet [7]	57.77	6.06	84.50	2.59
DTC [11]	56.90	7.39	84.29	2.36
URPC [12]	55.87	3.74	83.10	2.28
MC-Net [13]	62.85	2.33	86.44	1.82
SS-Net [25]	65.83	2.28	86.78	1.90
MCF [1]	82.37	1.59	87.67	2.08
BCP [10]	87.59	0.67	88.84	1.17
UCAD (ours)	88.63	0.49	89.93	0.57

Table 1. Comparison results with SoTA semi-supervised segmentation methods on ACDC dataset. Results of other methods are copied from BCP [10], while the results of ours are reproduced under the same setting.

Method	5% label		10% label	
	DSC(%) \uparrow	ASD \downarrow	DSC(%) \uparrow	ASD \downarrow
UA-MT [9]	31.96	61.16	40.63	37.77
URPC [12]	35.99	38.98	46.28	27.35
MC-Net [13]	36.70	52.13	43.89	35.78
CML [14]	36.52	54.51	58.49	41.30
BCP [10]	50.50	55.89	64.49	31.95
ABD [17]	51.28	39.45	62.41	24.22
UCAD (ours)	56.10	34.77	66.73	29.62

Table 2. Comparison results with SoTA semi-supervised segmentation methods on Synapse dataset.

GPU with fixed random seeds. And we set λ in Eq. 9 as 0.2. For evaluation, we utilize two widely used metrics: Dice Similarity Coefficient (DSC) and Average Surface Distance (ASD).

3.2. Comparison with State-of-the-art Methods

We compare the proposed method with several state-of-the-art (SoTA) semi-supervised medical image segmentation methods, including UA-MT [9], SASSNet [7], DTC [11], URPC [12], MC-Net [13], SS-Net [25], MCF [1], BCP [10], CML [14], and ABD [17] under 5% and 10% labeled settings, as summarized in Tables 1 and 2.

As shown in Table 1, our UCAD consistently outperforms all competitors on the ACDC dataset under both label ratios. With 5% labeled data, it achieves 88.63% DSC and 0.49 ASD, outperforming previous SoTA methods and demonstrating effective use of unlabeled data. When the label ratio increases to 10%, our method further improves to 89.93% DSC and 0.57 ASD, showing stable and robust consistency learning. Similarly, on the Synapse dataset (Table 2), our approach achieves the best results under both 5% and 10% labeled settings, with DSC gains of 4.82% and 2.24% over ABD.

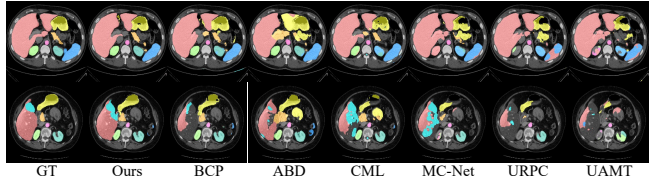


Fig. 3. Visual comparison on the 10% Synapse dataset: ■ spleen, ■ right kidney, ■ left kidney, ■ gallbladder, ■ pancreas, ■ liver, ■ stomach, and ■ aorta.

Base	CAD	UGS	\mathcal{L}_{unc}	DSC \uparrow	ASD \downarrow
✓				64.49	31.95
✓	✓			65.63	32.38
✓	✓	✓		66.38	29.69
✓	✓	✓	✓	66.73	29.62

Table 3. Ablation study on Synapse dataset with 10% labeled data. "Base" means using standard rectangular regions for displacement as the baseline. CAD means contour-aware displacement. UGS means adding uncertainty-guided selection in displacement. \mathcal{L}_{unc} means uncertainty-weighted consistency loss defined in Eq. 8.

The significant improvement on complex multi-organ CT scans highlights the advantage of our contour-aware mixing in preserving anatomical structures and refining boundaries.

3.3. Ablation Study

We conduct ablation experiments on the Synapse dataset using 10% labeled data to evaluate the contribution of each proposed component, as summarized in Table 3. Starting from the baseline model that adopts standard rectangular regions for displacement, introducing the contour-aware displacement (CAD) improves anatomical alignment and enhances boundary accuracy. Adding uncertainty-guided superpixel selection (UGS) further boosts performance by directing the displacement operations toward regions with low prediction confidence. Finally, integrating the uncertainty-weighted consistency loss \mathcal{L}_{unc} (Eq. 8) provides additional training stability by adaptively down-weighting unreliable pseudo-labels. The complete model achieves the best overall performance with a Dice score of 66.73% and an ASD of 29.62, demonstrating that all components work synergistically to achieve robust and shape-consistent semi-supervised segmentation.

4. CONCLUSION

In this paper, we proposed a novel uncertainty-guided contour-aware displacement framework UCAD. UCAD uses uncertainty to guide superpixels in generating anatomically aligned regions, incorporating shape awareness into input-level perturbations, and employs a dynamic uncertainty-weighted consistency loss to adaptively emphasize ambiguous regions and stabilize the learning process. Overall, UCAD achieves

remarkable results across extensive experiments, it provides a promising solution for semi-supervised medical image segmentation, with the potential to significantly improve segmentation accuracy under limited annotations.

5. COMPLIANCE WITH ETHICAL STANDARDS

Informed consent was obtained from all individual participants involved in the study.

6. ACKNOWLEDGMENTS

This work was supported by Natural Science Foundation of China under Grant 62271465 and Suzhou Basic Research Program under Grant SYG202338.

7. REFERENCES

- [1] Yongchao Wang, Bin Xiao, Xiuli Bi, Weisheng Li, and Xinbo Gao, “Mcf: Mutual correction framework for semi-supervised medical image segmentation,” in *CVPR*, 2023, pp. 15651–15660.
- [2] Fenghe Tang, Chengqi Dong, Wenxin Ma, Zikang Xu, Heqin Zhu, Zihang Jiang, Rongsheng Wang, Yuhao Wang, Chenxu Wu, and Shaohua Kevin Zhou, “U-bench: A comprehensive understanding of u-net through 100-variant benchmarking,” *arXiv preprint arXiv:2510.07041*, 2025.
- [3] Fenghe Tang, Bingkun Nian, Jianrui Ding, Wenxin Ma, Quan Quan, Chengqi Dong, Jie Yang, Wei Liu, and S Kevin Zhou, “Mobile u-vit: Revisiting large kernel and u-shaped vit for efficient medical image segmentation,” in *Proceedings of the 33rd ACM International Conference on Multimedia*, 2025, pp. 3408–3417.
- [4] Fenghe Tang, Wenxin Ma, Zhiyang He, Xiaodong Tao, Zihang Jiang, and Shaohua Kevin Zhou, “Pre-trained llm is a semantic-aware and generalizable segmentation booster,” in *International Conference on Medical Image Computing and Computer-Assisted Intervention*. Springer, 2025, pp. 402–412.
- [5] Fenghe Tang, Bingkun Nian, Yingtai Li, Zihang Jiang, Jie Yang, Wei Liu, and S Kevin Zhou, “Mambamim: Pre-training mamba with state space token interpolation and its application to medical image segmentation,” *Medical Image Analysis*, p. 103606, 2025.
- [6] Fenghe Tang, Ronghao Xu, Qingsong Yao, Xueming Fu, Quan Quan, Heqin Zhu, Zaiyi Liu, and S Kevin Zhou, “Hyspark: Hybrid sparse masking for large scale medical image pre-training,” in *International Conference on Medical Image Computing and Computer-Assisted Intervention*. Springer, 2024, pp. 330–340.
- [7] Shuailin Li, Chuyu Zhang, and Xuming He, “Shape-aware semi-supervised 3d semantic segmentation for medical images,” in *MICCAI*. Springer, 2020, pp. 552–561.
- [8] Antti Tarvainen and Harri Valpola, “Mean teachers are better role models: Weight-averaged consistency targets improve semi-supervised deep learning results,” *NeurIPS*, vol. 30, 2017.
- [9] Lequan Yu, Shujun Wang, Xiaomeng Li, Chi-Wing Fu, and Pheng-Ann Heng, “Uncertainty-aware self-ensembling model for semi-supervised 3d left atrium segmentation,” in *MICCAI*. Springer, 2019, pp. 605–613.
- [10] Yunhao Bai, Duowen Chen, Qingli Li, Wei Shen, and Yan Wang, “Bidirectional copy-paste for semi-supervised medical image segmentation,” in *CVPR*, 2023, pp. 11514–11524.
- [11] Xiangde Luo, Jieneng Chen, Tao Song, and Guotai Wang, “Semi-supervised medical image segmentation through dual-task consistency,” in *AAAI*, 2021, vol. 35, pp. 8801–8809.
- [12] Xiangde Luo, Wenjun Liao, Jieneng Chen, et al., “Efficient semi-supervised gross target volume of nasopharyngeal carcinoma segmentation via uncertainty rectified pyramid consistency,” in *MICCAI*. Springer, 2021, pp. 318–329.
- [13] Yicheng Wu, Minfeng Xu, Zongyuan Ge, Jianfei Cai, and Lei Zhang, “Semi-supervised left atrium segmentation with mutual consistency training,” in *MICCAI*. Springer, 2021, pp. 297–306.
- [14] Song Wu, Xiaoyu Wei, Xinyue Chen, Yazhou Ren, Jing He, and Xiaorong Pu, “Cross-view mutual learning for semi-supervised medical image segmentation,” in *ACM MM*, 2024, pp. 9253–9261.
- [15] Lihe Yang, Zhen Zhao, and Hengshuang Zhao, “Unimatch v2: Pushing the limit of semi-supervised semantic segmentation,” *TPAMI*, 2025.
- [16] Fenghe Tang, Jianrui Ding, Lingtao Wang, Min Xian, and Chunping Ning, “Multi-level global context cross consistency model for semi-supervised ultrasound image segmentation with diffusion model,” *arXiv preprint arXiv:2305.09447*, 2023.
- [17] Hanyang Chi, Jian Pang, Bingfeng Zhang, and Weifeng Liu, “Adaptive bidirectional displacement for semi-supervised medical image segmentation,” in *CVPR*, 2024, pp. 4070–4080.

- [18] Ashwin Raju, Shun Miao, Dakai Jin, Le Lu, Junzhou Huang, and Adam P Harrison, “Deep implicit statistical shape models for 3d medical image delineation,” in *AAAI*, 2022, vol. 36, pp. 2135–2143.
- [19] Radhakrishna Achanta, Appu Shaji, Kevin Smith, et al., “Slic superpixels compared to state-of-the-art superpixel methods,” *TPAMI*, vol. 34, no. 11, pp. 2274–2282, 2012.
- [20] Claude E Shannon, “A mathematical theory of communication,” *The Bell system technical journal*, vol. 27, no. 3, pp. 379–423, 1948.
- [21] Maregu Assefa, Muzammal Naseer, Iyyakutti Iyappan Ganapathi, et al., “Dycon: Dynamic uncertainty-aware consistency and contrastive learning for semi-supervised medical image segmentation,” in *CVPR*, 2025, pp. 30850–30860.
- [22] Olivier Bernard, Alain Lalande, Clement Zotti, Frederick Cervenansky, Xin Yang, Pheng-Ann Heng, Irem Cetin, Karim Lekadir, Oscar Camara, Miguel Angel Gonzalez Ballester, et al., “Deep learning techniques for automatic mri cardiac multi-structures segmentation and diagnosis: is the problem solved?,” *TMI*, vol. 37, no. 11, pp. 2514–2525, 2018.
- [23] Bennett Landman, Zhoubing Xu, Juan Iglesias, Martin Styner, Thomas Langerak, and Arno Klein, “Miccai multi-atlas labeling beyond the cranial vault—workshop and challenge,” in *Proc. MICCAI multi-atlas labeling beyond cranial vault—workshop challenge*. Munich, Germany, 2015, vol. 5, p. 12.
- [24] Olaf Ronneberger, Philipp Fischer, and Thomas Brox, “U-net: Convolutional networks for biomedical image segmentation,” in *MICCAI*. Springer, 2015, pp. 234–241.
- [25] Yicheng Wu, Zhonghua Wu, Qianyi Wu, Zongyuan Ge, and Jianfei Cai, “Exploring smoothness and class-separation for semi-supervised medical image segmentation,” in *MICCAI*. Springer, 2022, pp. 34–43.